



Thiophene Derivatives as Corrosion Inhibitors for CS in 0.5 M H₂SO₄ Solutions

A.S.Fouda^{1*}, S. Abd El-Maksoud², S.A. Gomaa³ and A.Elsalakawy³

1. Department of Chemistry, Faculty of ScPEnce, El-Mansoura University, **EGYPT**
2. Department of Chemistry, Faculty of ScPEnce, Port Said University, Port Said, **EGYPT**
3. El-Delta Company for Fertilizer and Chemicals, Talkha, El-Daqahlia, **EGYPT**

Email: asfouda@hotmail.com

Accepted on 13th January 2017, Published online on 27th January 2017

ABSTRACT

Some thiophene derivatives were tested as corrosion inhibitors for CS (CS) in 0.5 M H₂SO₄ at room and higher temperatures. Different methods were used to determine the protection efficiency (PE), such as weight loss (WL), potentiodynamic polarization (PP), electrochemical impedance spectroscopy (EIS) and electrochemical frequency modulation (EFM). The results showed the variation in inhibition performance of the inhibitors with varying doses and temperatures. The maximum efficiency was found to be 91 % at 2x10⁻⁴ M of the inhibitors for the immersion period of 3 hours. Langmuir was tested to describe the adsorption behavior of inhibitor on CS surface. PP study clearly revealed that these compounds act as mixed type inhibitors. The results of the EIS study showed a decrease in double layer capacitance (C_{dl}) and increase in charge transfer resistance (R_{ct}). The results of various electrochemical techniques show good agreements with each other and with WL method.

Keywords: Thiophene derivatives, Corrosion inhibition, H₂SO₄, CS, PP, WL, EIS, EFM.

INTRODUCTION

Thiophene derivatives [1] find large applications in material science [2-12], in coordination chemistry [13,14] and as intermediate in organic synthesis [15,16]. Presence of hetero atoms such as O, N, S in thiophene derivatives encourage us to use it as corrosion inhibitors [17-20] due to overlapping of P orbital of hetero atoms with vacant d orbital of metal [21-29]. CS used in multi industries processes and multi usage so, we apply our study on this metal. Corrosion study easier in acidic medium so, all investigation of corrosion behavior carried on 0.5 M of H₂SO₄. With regard to CS corrosion in acid medium, a lot of investigations in relation to pickling, acid cleaning, the study of corrosion inhibition has been reported [30]. The mechanism of corrosion inhibition is involved with the formation of protective film resulted from organic molecules adsorption on the surface of metal from the environment bulk [31]. Since this inhibitor contains sulfur atom and the methyl group in thiophene has induction effect related to increased electron density of donor atom.

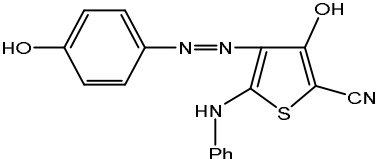
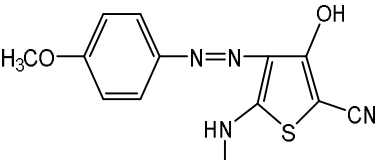
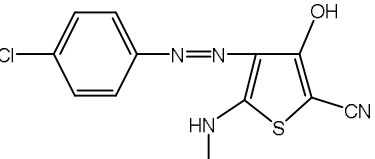
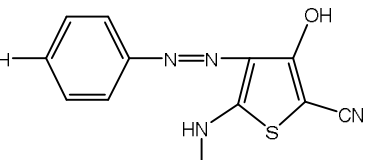
Several studies concerning the corrosion inhibition of Al by organic compounds in acidic solutions have been conducted [32-35]. Recent studies have been performed with the effects of sulfur-containing compounds such as thiourea and its derivatives on the inhibition of Al corrosion [36]. Most organic inhibitors act by adsorption on the metal surfaces [37].

In the present work, chemical method was used to investigate the inhibition of Al corrosion by some thiophene derivatives in 0.5 M H₂SO₄, with respect to the effects of inhibitor concentration and temperature on the inhibitor efficiency (PE %).

MATERIALS AND METHODS

Materials: The CS samples are taken from the same sheet of the following Composition in weight %: C 0.08 – 0.13, Mn 0.3-0.6, P < 0.04, S < 0.05 and Fe balance. All chemicals were used in analytical grade A. Ethanol with 99.7% purity was purchased from Hayman Ltd., while acetone and sulphuric acid (H₂SO₄) with 98% purity were ordered from El-Gomhoria Company, Mansoura, Egypt. This study used CS coupon with a size of 20 x 20 x 2 mm. A WL method was used to determine the PE based on the CS weights in the nonexistence and existence of thiophene derivatives as inhibitors. Chemical structures, names, molecular weights and molecular formulas of thiophene derivatives [38] are shown in table 1.

Table 1. Chemical structures, names, molecular weights and molecular formulas of thiophene derivatives

Name	Structure and IUPAC name	Chemical Formula	Mol. Wt
A	 3-hydroxy-4-((4-hydroxyphenyl)diazenyl)-5-(phenylamino)thiophene-2-carbonitrile	C ₁₇ H ₁₂ N ₄ O ₂ S	336.37
B	 3-hydroxy-4-((4-methoxyphenyl)diazenyl)-5-(phenylamino)thiophene-2-carbonitril	C ₁₈ H ₁₄ N ₄ O ₂ S	350.39
C	 4-((4-chlorophenyl)diazenyl)-3-hydroxy-5-(phenylamino)thiophene-2-carbonitrile	C ₁₇ H ₁₁ ClN ₄ OS	354.81
D	 4-((4-formylphenyl)diazenyl)-3-hydroxy-5-(phenylamino)thiophene-2-carbonitrile	C ₁₈ H ₁₂ N ₄ O ₂ S	348.38

WL analysis: Six CS specimen of the dimensions 2 x 2 x 0.2 cm were polished to mirror finish, with emery papers (a coarse paper was used initially and then progressively finer grades were employed), degreased in acetone, rinsed with bi distilled water and finally dried between two filter papers and used in W_1 and surface examination studies. The test pieces were suspended by suitable glass hooks at the edge of the basin, and under the surface of the test solution by about 1 cm. WL measurements were performed for 3 hours at the temperature range from 25 – 55°C by dipping CS pieces into 100 mL acid solution with and without various doses of inhibitors. After the specified periods of time, the specimen were taken out of the test solution, rinsed with bi distilled water, dried as before and weighed again accurately. The average weight loss at a certain time for each set of the six samples was taken. The weight loss was recorded to nearest 0.0001 g.

Electrochemical experiments were performed using a typical three-compartment glass cell consisted of the CS specimen as working electrode. The CS rod encapsulated in Teflon with an exposed cross section of a 1 cm² diameter. Saturated calomel electrode (SCE) was used as a reference electrode and a platinum foil as a counter electrode. The reference electrode was connected to a Luggin capillary and the tip of the Luggin capillary is made very close to the surface of the working electrode to minimize IR drop. All the measurements were done in solutions open to atmosphere under unstirred conditions. All potential values were reported versus SCE. Prior to every experiment, the electrode was abraded with successive different grades of emery paper, degreased with acetone and washed with bi distilled water and finally dried.

PP curves were obtained by changing the electrode potential automatically from (-0.5 to 0.5 V vs. SCE) at open circuit potential with a scan rate of 1 mVs⁻¹. The corrosion current is performed by extrapolation of anodic and cathodic Tafel lines to a point which gives log i_{corr} and the corresponding corrosion potential (E_{corr}) for inhibitor free acid and for each concentration of inhibitor.

EIS were carried out in frequency range from 100 kHz to 0.1Hz with amplitude of 5 mV peak-to-peak using ac signals at open circuit potential. The experimental impedance was analyzed and interpreted based on the equivalent circuit. The main parameters deduced from the analysis of Nyquist diagram are the charge transfer resistance R_{ct} (diameter of high-frequency loop) and the double layer capacity C_{dl} .

EFM was carried out using two frequencies 2 and 5Hz. The base frequency was 0.1 Hz, so the waveform repeats after 1s. The higher frequency must be at least two times the lower one. The higher frequency must also be sufficiently slow that the charging of the double layer does not contribute to the current response, often 10 Hz is a reasonable limit. The Inter modulation spectra contain current responses assigned for harmonical and inter modulation current peaks. The larger peaks were used to calculate the corrosion current density (i_{corr}), the Tafel slopes (β_c and β_a) and the causality factors CF-2 and CF-3 All electrochemical measurements were performed using Gamry Instrument (PCI 300/4)Potentiostat / Galvanostat /ZRA. This includes Gamry applications, DC105 software for DC corrosion, EIS300 software for EIS, and EFM140 for measurements along with a computer for collecting data. E chem. analyst v 6.03 software was used for plotting, graphing, and fitting data.

Thermodynamic study: The thermodynamic investigation is necessary to perceive the type of interaction between inhibitor and metal surface in the adsorption process of methyl thiophene inhibition. Parameters such as temperature, K_{ads} and ΔG°_{ads} are required for thermodynamic investigation. The value of ΔG°_{ads} (change of Gibbs free energy for adsorption) is an indicator to determine the type of interaction between inhibitor and metal surface whether it shows a chemical or physical adsorption. The value of K_{ads} as the equilibrium constant obtained from the proposed model of isotherm adsorption can be assumed as the K_{ads} required in the thermodynamic study [39].The thermodynamic expression required to perform the type of adsorption in relation to corrosion inhibition is described as follows:

$$\Delta G^{\circ}_{ads} = - RT \ln(55.5 K_{ads})$$

($R = 8.314 \text{ J mol}^{-1} \text{ K}^{-1}$; $T = \text{temperature}$; $55.5 = \text{concentration of water (mol/L) in solution}$)

RESULTS AND DISCUSSION

WL method: Figure 1 shows plots for the variation of weight loss of CS with time in 0.5 M H₂SO₄ containing various doses of compound (A) at 25°C. Similar curves were obtained for other inhibitor but not shown. From the plots; it is evident that the weight loss of CS was also found to decrease with rise in the dose of compound (A).

The WL of CS in the blank solution was also found to be higher than those obtained for solutions of H₂SO₄ containing various doses of are presented. The degree of surface coverage (θ) and % PE were calculated using equation (1):

$$\% PE = \theta \times 100 = [1 - (CR_{inh} / CR_{free})] \times 100 \quad (1)$$

Where CR_{inh} and CR_{free} are the corrosion rates in the nonexistence and existence of inhibitor respectively. CR and % PE at different doses of inhibitors for the corrosion of CS after 120 min immersion in 0.5 M H₂SO₄ at 25 °C are shown in Table 2. It can be seen that the maximum of 90.8% inhibition efficiency is achieved at 2x10⁻⁴M of inhibitor dose and % PE increases with increasing the inhibitor doses. This is mainly due to the active chemical constituent of viz, π bonds, hetero atoms (O and N). The almost greater than 90% of θ is due to the co-ordination between the metal and the hetero atom present in the inhibitor. From the calculated values of %PE, the order of the PE of inhibitors was as follows: A > B > C > D. This indicates that compound A is the more adsorbed inhibitor for the corrosion of CS in solutions of H₂SO₄.

Table 2. CR and %PE at different doses of inhibitors for the corrosion of CS after 120 min immersion in 0.5M H₂SO₄ at 25 °C

Conc. [M]x 10 ⁵	Inhibitor A		Inhibitor B		Inhibitor C		Inhibitor D	
	C.R mg cm ⁻² min ⁻¹	% PE	C.R mg cm ⁻² min ⁻¹	% PE	C.R mg cm ⁻² min ⁻¹	% PE	C.R mg cm ⁻² min ⁻¹	% PE
0	5.24	--	5.24	--	5.24	--	5.24	--
4	1.95	62.5	1.94	62.8	2.47	52.8	4.38	16.2
8	1.49	71.3	1.65	68.4	2.11	59.7	3.65	30.2
12	1.08	79.3	1.43	72.5	1.75	66.6	3.13	40.1
16	0.85	83.6	1.24	76.1	1.6	69.4	2.62	49.8
20	0.71	86.4	1.11	78.6	1.43	72.7	2.21	57.6
24	0.47	90.8	1.00	80.7	1.20	76.9	1.90	63.5

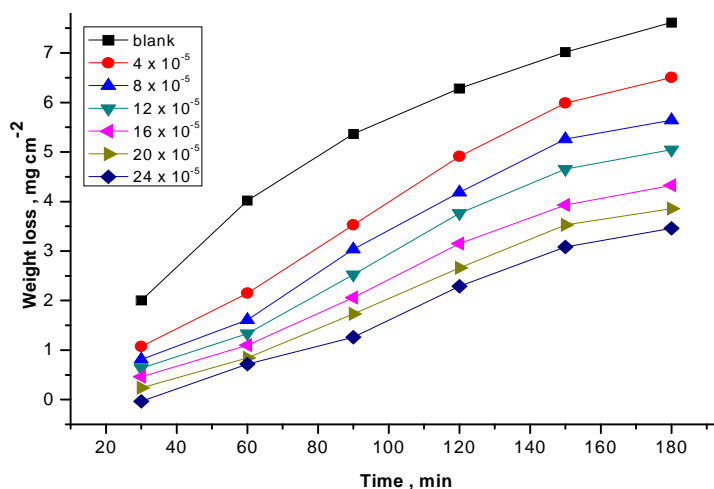


Figure 1. Weight loss-time curves for the corrosion of CS in 0.5 M H₂SO₄ in the absence and presence of different doses of inhibitor A at 25°C

Effect of temperature on inhibition efficiency (% PE): The inhibition efficiency (% PE) for CS corrosion in the presence of various doses of the investigated thiophene derivatives and at different temperatures was calculated and is listed in table 3. The results of table 3 illustrate the variation of CR and %PE with inhibitors doses at different temperatures. The obtained data revealed that, the PE decreased with an increase in the inhibitor dose. This suggests that the inhibitor species are adsorbed on the CS solution interface where the adsorbed species mechanically form a protected film on the metal surface which inhibits the action of the corrosion. A close comparison between tables 2 and 3 revealed that WL of CS increases with increasing temperature indicating that the rate of corrosion of CS increases with increase in temperature. The value of inhibition efficiency was decreased with rise in temperature suggests that physical adsorption mechanism [40]. These results indicate that the adsorption of investigated compounds shield the metal surface at room temperature [41]. However it may be shielded from the surface with rise in temperature. It is also clear that CR of CS in the nonexistence and existence of inhibitors obeys Arrhenius type equation as it increases with raising solution temperature. The dependence of CR (i_{corr}) on the temperature can be expressed by Arrhenius equation 2:

$$i_{\text{corr}} = A \exp^{(-E_a^*/RT)} \quad (2)$$

Where A is the pre-exponential factor and E_a^* is the apparent activation energy of the corrosion process. Arrhenius plot obtained for the corrosion of CS in 0.5 M sulphuric acid solutions in the existence of different doses of compound A) is shown in figure 2. E_a^* values determined from the slopes of these linear plots are shown in table 4. The linear regression (R^2) is close to 1 which indicates that the corrosion of CS in 0.5 M sulphuric acid solutions can be elucidated using the kinetic model. Table 4 showed that the values of E_a^* for inhibited solution is higher than that for uninhibited solution, suggesting that dissolution of CS is slow in the presence of inhibitor. It is known from Eq. 2 that the higher E_a^* values lead to the lower CR. This is due to the formation of a film on the CS surface serving as an energy barrier for the CS corrosion. Enthalpy and entropy of activation (ΔH^* , ΔS^*) of the corrosion process were calculated from the transition state theory as given from equation 3 and shown in table 4:

$$k_{\text{corr}} = (RT/Nh) \exp(\Delta S^*/R) \exp(-\Delta H^*/RT) \quad (3)$$

Where h is Planck's constant and N is Avogadro's number. A plot of $\log(k_{\text{corr}}/T)$ vs. $1/T$ for CS in 0.5 M sulphuric acid with different doses of compound (A) gives straight lines as shown in figure 3. Similar curves were obtained for other compounds but not shown. Values of ΔH^* are positive. This indicates that the corrosion process is an endothermic one. The entropy of activation ΔS^* is large and negative. This implies that the activated complex represents association rather than dissociation step, indicating that a decrease in disorder takes place, going from reactants to the activated complex [42].

Table 3. Variation of % PE and CR for various doses of the studied inhibitors at different temperatures

Temp °C	Conc. [M] x 10 ⁵	Inhibitor A		Inhibitor B		Inhibitor C		Inhibitor D	
		C.R mg cm ⁻² min ⁻¹	% PE	C.R mgcm ⁻² min ⁻¹	% PE	C.R mgcm ⁻² min ⁻¹	% PE	C.R mgcm ⁻² min ⁻¹	% PE
25	0	5.24	--	5.24	--	5.24	--	5.24	--
	4	1.95	62.5	1.94	62.8	2.47	52.8	4.38	16.2
	8	1.49	71.3	1.65	68.4	2.11	59.7	3.65	30.2
	12	1.08	79.3	1.43	72.5	1.75	66.6	3.13	40.1
	16	0.85	83.6	1.24	76.1	1.6	69.4	2.62	49.8
	20	0.71	86.4	1.11	78.6	1.43	72.7	2.21	57.6
	24	0.47	90.8	1.00	80.7	1.20	76.9	1.90	63.5
35	0	10.24	--	10.24	--	10.24	--	10.24	--
	4	4.67	54.3	2.53	75.2	3.83	62.6	7.95	13.9
	8	3.71	63.7	2.02	80.1	2.96	71.1	7.41	25.2

	12	2.81	72.5	1.93	81.1	2.58	74.8	6.72	34.4
	16	2.31	77.3	1.82	82.2	1.97	80.7	5.83	43.1
	20	2.02	80.2	1.57	84.6	1.74	83.0	5.01	51.0
	24	1.38	86.5	1.43	86.0	1.43	86.0	3.98	58.8
45	0	19.68	--	19.67	--	19.67	--	19.68	--
	4	11.12	43.4	5.42	72.4	5.51	71.9	16.34	11.5
	8	8.98	54.3	4.80	75.5	4.28	78.2	14.81	21.7
	12	7.04	64.2	4.28	78.2	3.19	83.7	13.55	31.1
	16	5.67	71.1	3.88	80.2	2.57	86.9	11.76	40.2
	20	4.95	74.7	3.49	82.2	2.10	89.3	9.76	49.1
	24	3.59	81.7	2.99	84.7	1.57	91.9	8.39	57.3
55	0	35.27	--	35.27	--	35.27	--	35.27	--
	4	25.24	28.4	11.63	67.0	8.81	75.0	31.52	10.1
	8	20.73	41.2	9.37	73.4	5.45	84.5	28.45	19.4
	12	16.87	52.1	8.01	77.3	4.60	86.9	25.12	28.4
	16	14.41	59.1	7.02	80.1	3.24	90.7	21.98	37.5
	20	12.44	64.7	6.14	82.5	2.67	92.4	19.71	44.9
	24	11.39	67.7	5.51	84.3	1.95	94.4	16.63	52.6

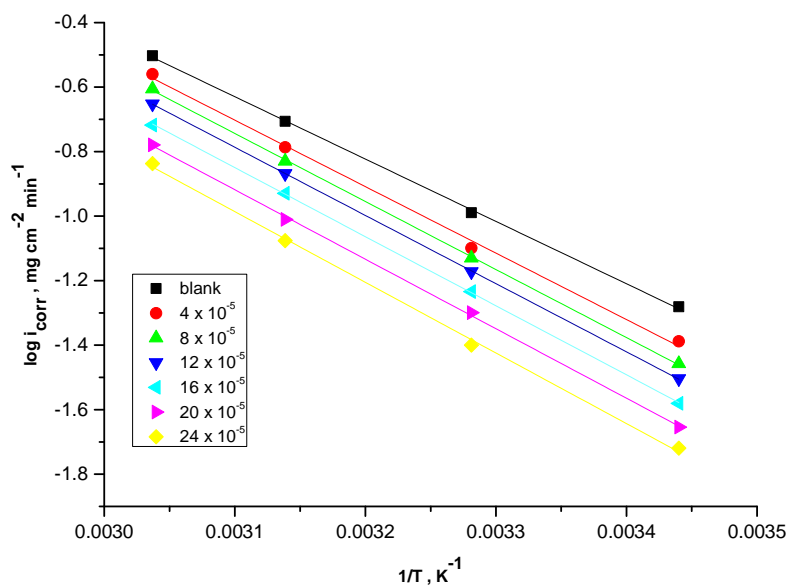


Figure 2. Arrhenius plots for CS rates (i_{corr}) after 120 minute of immersion in 0.5 M H_2SO_4 in the nonexistence and existence of various doses of inhibitor A

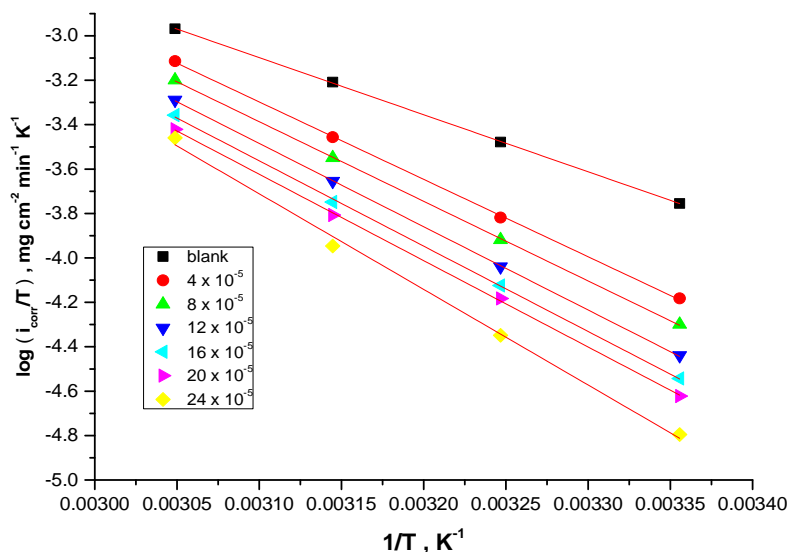


Figure 3. Log i_{corr}/T vs. $1/T$ for CS corrosion after 120 minute of immersion in 0.5 M H_2SO_4 in the nonexistence and existence of various doses of inhibitor A

Table 4. Activation parameters for CS surface corrosion in the nonexistence and existence of various doses of investigated inhibitors in 0.5 M H_2SO_4

Inhibitor	Conc $\times 10^5$ M	Activation parameters		
		E_a^* kJ mol^{-1}	ΔH^* kJ mol^{-1}	$-\Delta S^*$ $\text{J mol}^{-1} \text{K}^{-1}$
Blank	0.0	51.9	21.4	104.2
A	4	69.3	29.0	53.8
	8	71.3	29.8	49.6
	12	74.4	31.2	41.7
	16	76.2	32.0	37.7
	18	77.1	32.3	36.0
	20	85.0	35.8	13.1
	24	69.3	29.0	53.8
B	4	49.5	20.4	121.7
	8	49.1	20.2	124.6
	12	48.2	19.8	128.3
	16	48.1	19.8	129.5
	18	47.91	19.67	131.1
	20	47.30	19.41	134.0
	24	49.49	20.36	121.7
C	4	33.95	13.61	170.6
	8	26.17	10.23	197.8
	12	25.30	9.86	202.3
	16	19.39	7.29	223.1
	18	16.79	6.16	232.7
	20	12.49	4.29	248.5
	24	33.95	13.61	170.6
D	4	53.90	22.27	99.1
	8	55.68	23.04	94.4
	12	56.49	23.40	92.7
	16	57.58	23.87	90.5
	18	58.72	24.37	88.1
	20	58.86	24.43	89.1
	24	53.90	22.27	99.1

Adsorption isotherms: Adsorption isotherm values are important to explain the mechanism of PE of organo-electrochemical reactions. The most frequently used isotherms are Langmuir isotherm (Figure 4). Figure 5 shows $\log K_{\text{ads}}$ vs. $1/T$ for the corrosion of CS in 0.5 M H_2SO_4 in the existence of different inhibitors. Thermodynamic parameters for the adsorption of different inhibitors on CS surface in 0.5 M H_2SO_4 at different temperatures was listed in table 5.

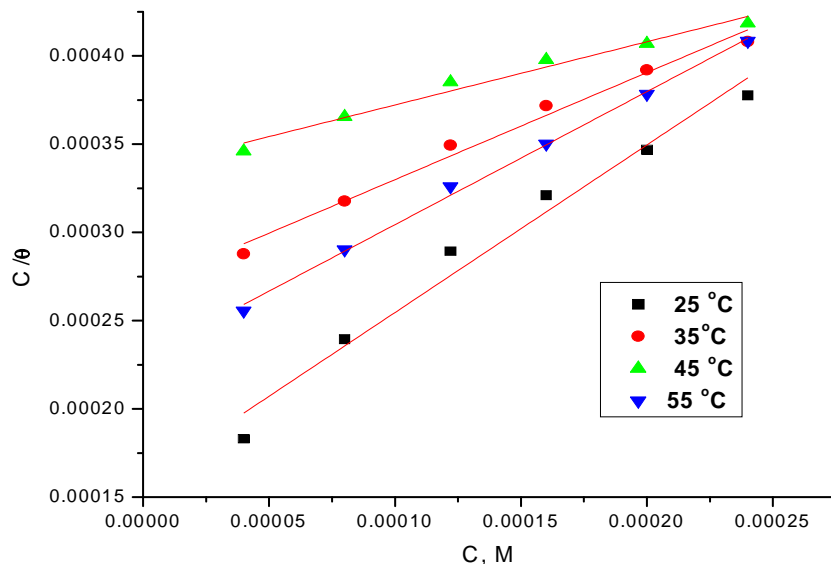


Figure 4. Langmuir adsorption isotherm of inhibitor (A) on CS in 0.5 M H_2SO_4 at different temperatures

Table 5. Thermodynamic adsorption parameters for the adsorption of thiophene derivatives on CS in 0.5 M sulphuric acid at different temperatures

Inhibitor	Temp °C	K_{ads} M^{-1}	$-\Delta G_{\text{ads}}^{\circ}$ kJ mol^{-1}	$-\Delta H_{\text{ads}}^{\circ}$ kJ mol^{-1}	$-\Delta S_{\text{ads}}^{\circ}$ $\text{J mol}^{-1} \text{K}^{-1}$
A	25	34.33	35.8	34.5	4.6
	35	25.07	36.	34.5	5.7
	45	16.29	36.3	34.5	5.6
	55	9.58	36.0	34.5	4.5
B	25	45.13	36.5	25.7	36.2
	35	101.20	39.8	25.7	45.7
	45	73.48	40.2	25.7	45.7
	55	54.85	40.7	25.7	45.7
C	25	28.03	35.3	24.4	36.2
	35	38.50	37.3	24.4	45.7
	45	54.34	39.5	24.4	45.7
	55	67.99	41.3	24.4	45.7
D	25	46.19	30.9	16.0	49.9
	35	37.11	31.3	16.0	49.8
	45	29.60	31.8	16.0	49.6
	55	25.88	32.4	16.0	49.9

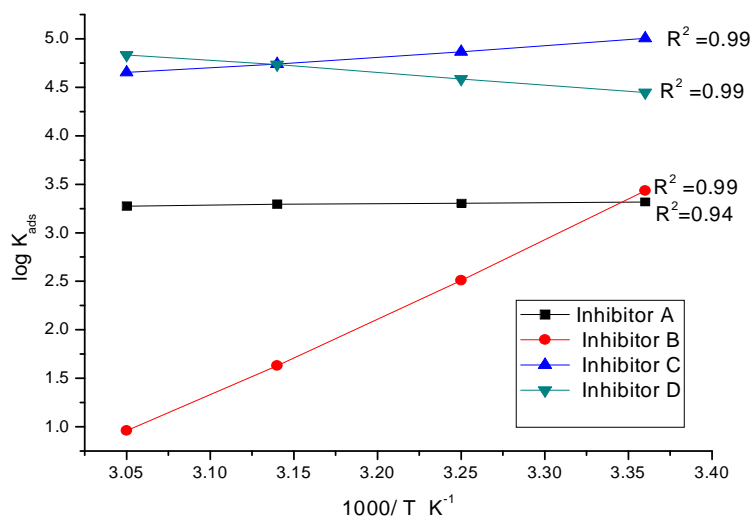


Figure 5. Log K_{ads} vs. $1/T$ for the corrosion of CS in 0.5 M H_2SO_4 in the presence of different inhibitors

From table 5 it was found that the negative values of $\Delta G_{\text{ads}}^{\circ}$ reflect that the adsorption of studied thiophene derivatives on CS in 0.5 M H_2SO_4 solution is spontaneous process [43]. $\Delta G_{\text{ads}}^{\circ}$ values increase (become less negative) with an increase of temperature which indicates the occurrence of exothermic process at which adsorption was unfavorable with increasing reaction temperature as the result of the inhibitor desorption from the CS surface [44]. It is usually accepted that the value of $\Delta G_{\text{ads}}^{\circ}$ around -20 kJ mol^{-1} or lower indicates the electrostatic interaction between charged metal surface and charged organic molecules in the bulk of the solution [45]. The negative sign of $\Delta H_{\text{ads}}^{\circ}$ reveals that the adsorption of inhibitor molecules is an exothermic process. Generally, an exothermic adsorption process suggests either physisorption or chemisorptions while endothermic process is attributed to chemisorptions [46]. Generally, enthalpy values upto 41.9 kJ mol^{-1} are related to the electrostatic interactions between charged molecules and charged metal (physisorption) while those around 100 kJ mol^{-1} or higher are attributed to chemisorptions. The unshared electron pairs in investigated molecules may interact with d orbitals of Fe to provide a protective chemisorbed film [47]. In the case of investigated compounds; the absolute values of enthalpy are relatively low, approaching those typical of physisorption. The values of $\Delta S_{\text{ads}}^{\circ}$ in the presence of investigated compounds are large and negative that is accompanied with exothermic adsorption process [48]. The experimental data give good curves fitting for the applied adsorption isotherm as the correlation coefficients (R^2) were in the range 0.950-0.997. K_{ads} value decreases with the increase of temperature from 25 to 55°C.

PP measurements: Polarization measurements were carried out in order to gain knowledge concerning the kinetics of the cathodic and anodic reactions. Figure 6 presents the results of the effect of compound (A) on the cathodic and anodic polarization curves of CS in 0.5 M H_2SO_4 . Similar curves for other compounds were obtained but not shown. It could be observed that both the cathodic and anodic reactions were suppressed with the addition of investigated compounds, which suggested that these compounds reduced anodic dissolution and also retarded the hydrogen evolution reaction. Electrochemical corrosion kinetics parameters, i.e. corrosion potential (E_{corr}), cathodic and anodic Tafel slopes (β_a , β_c) and corrosion current density (i_{corr}) obtained from the extrapolation of the polarization curves were given in Table 6. The parallel cathodic Tafel curves in Figure 6 suggested that the hydrogen evolution is activation-controlled and the reduction mechanism is not affected by the presence of the inhibitor. The region between linear part of cathodic and anodic branch of polarization curves becomes wider as the inhibitor is added to the acid solution. Similar results were found in the literature⁽⁴⁴⁾. The values of β_a and β_c changed slightly with increasing inhibitor concentration indicated the influence of these compounds on the kinetics of metal dissolution and of hydrogen evolution. Due to the presence of some active sites, such as aromatic rings,

hetero-atoms in the studied compound for making adsorption, they may act as adsorption inhibitors. Being absorbed on the metal surface, these compounds controlled the anodic and cathodic reactions during corrosion process, and then their corrosion inhibition efficiencies are directly proportional to the amount of adsorbed inhibitor. The functional groups and structure of the inhibitor play important roles during the adsorption process. On the other hand, an electron transfer takes place during adsorption of the neutral organic compounds at metal surface [49]. As it can be seen from Table 6, the studied inhibitor reduced both anodic and cathodic currents with a slight shift in corrosion potential (47 mV). According to Ferreira and others [50], if the displacement in corrosion potential is more than 85 mV with respect to corrosion potential of the blank solution, the inhibitor can be seen as a cathodic or anodic type. In the present study, the displacement was 44 mV which indicated that the studied inhibitor is mixed type inhibitor. The results obtained from PP showed good agreement with the results obtained from WL method. The θ and % PE were calculated using equation 4.

$$\%PE = \theta \times 100 = [1 - (i_{\text{corr}}/i_{\text{corr}}^{\circ})] \times 100 \quad (4)$$

Where i_{corr} and i_{corr}° are the current densities in presence and absence of inhibitor, respectively.

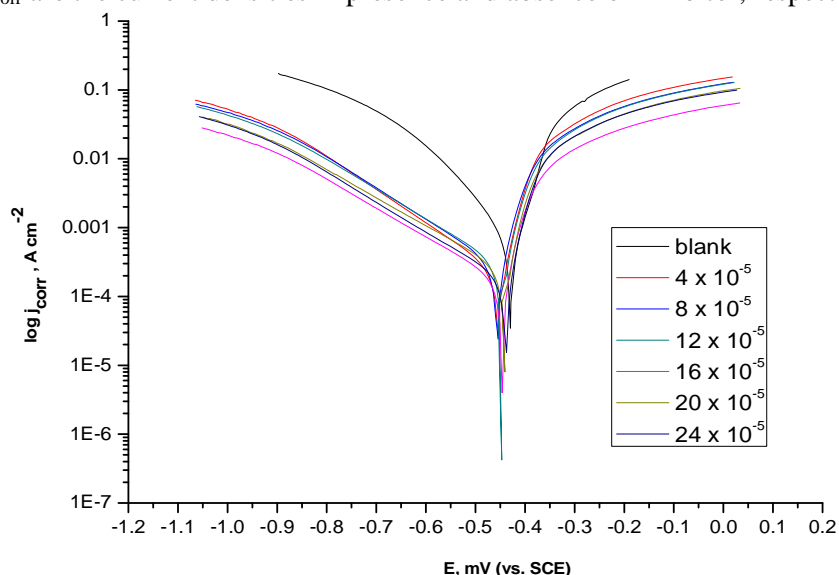


Figure 6. PP plots for the dissolution of CS in 0.5 M H₂SO₄ in the nonexistence and existence of different doses of compound (A) at 25°C

Table 6: Effect of doses of various compounds on the E_{corr} , i_{corr} , β_c , β_a , CR, θ and %PE of CS in (0.5 M) H₂SO₄

Inhibitor	Conc. M $\times 10^5$	$-E_{\text{corr}}$ vs SCE, mV	i_{corr} , $\mu\text{A cm}^{-2}$	β_a , mV dec^{-1}	β_c , mV dec^{-1}	C.R.	θ	% PE
Blank	0.0	429	770	61	135	351.7		
A	4	461	393	202	51	179.7	0.490	49.0
	8	462	364	214	53	166.5	0.527	52.7
	12	465	359	190	59	164.2	0.534	53.4
	16	441	213	242	59	97.50	0.723	72.3

	20	440	201	142	50	91.66	0.739	73.9
	24	451	125	256	73	57.26	0.838	83.8
B	4	456	312	55	225	142.6	0.559	59.5
	8	447	292	56	231	133.6	0.621	62.1
	12	441	236	48	243	107.8	0.694	69.4
	16	453	217	44	202	99.27	0.718	71.8
	20	446	180	58	245	82.11	0.766	76.6
	24	439	172	40	230	78.65	0.777	77.7
C	4	452	390	240	60	178.4	0.494	49.4
	8	447	340	273	80	155.3	0.558	55.8
	12	454	239	247	57	109.1	0.690	69.0
	16	456	213	220	50	97.14	0.723	72.3
	20	450	207	247	54	94.42	0.731	73.1
	24	452	205	233	57	93.45	0.734	73.4
D	4	472	534	54	181	243.9	0.306	30.6
	8	473	401	61	186	183.4	0.479	47.9
	12	466	370	46	167	169.3	0.519	51.9
	16	464	330	49	177	150.6	0.571	57.1
	20	466	321	49	185	146.6	0.583	58.3
	24	461	311	44	181	142.2	0.596	59.6

EIS Measurements: Nyquist and Bode plots of CS in uninhibited and inhibited acid solutions containing different doses of compound (A) are presented in figures 7, 8 respectively. EIS spectra obtained consists of one depressed capacitive loop (one time constant in Bode-phase plot). The increased diameter of capacitive loop obtained in 0.5 M H₂SO₄ in presence of compound (A) indicated the PE of CS. The high frequency capacitive loop may be attributed to the charge transfer reaction. Corrosion kinetic parameters

derived from EIS measurements and PE are given in Table 7. Double layer capacitance (C_{dl}) and charge transfer resistance (R_{ct}) were obtained from EIS measurements as described elsewhere [51]. This decrease in C_{dl} results from a decrease in local dielectric constant and/or an increase in the thickness of the double layer, suggested that inhibitor molecules inhibit the CS corrosion by adsorption at the metal/acid interface [52]. The depression in Nyquist semicircles is a feature for solid electrodes and often referred to as frequency dispersion and attributed to the roughness and other in homogeneities of the solid electrode [53]. Figure 9 showed the electrical equivalent circuit employed to analyze the impedance spectra. Excellent fit with this model was obtained for all experimental data. The surface coverage (θ) and % PE were calculated using equation 6:

$$\%PE = \theta \times 100 = [1 - (R_{ct}/R_{ct}^{\circ})] \times 100 \quad (6)$$

Where R_{ct} and R_{ct}° are the charge transfer resistances in absence and presence of inhibitor, respectively

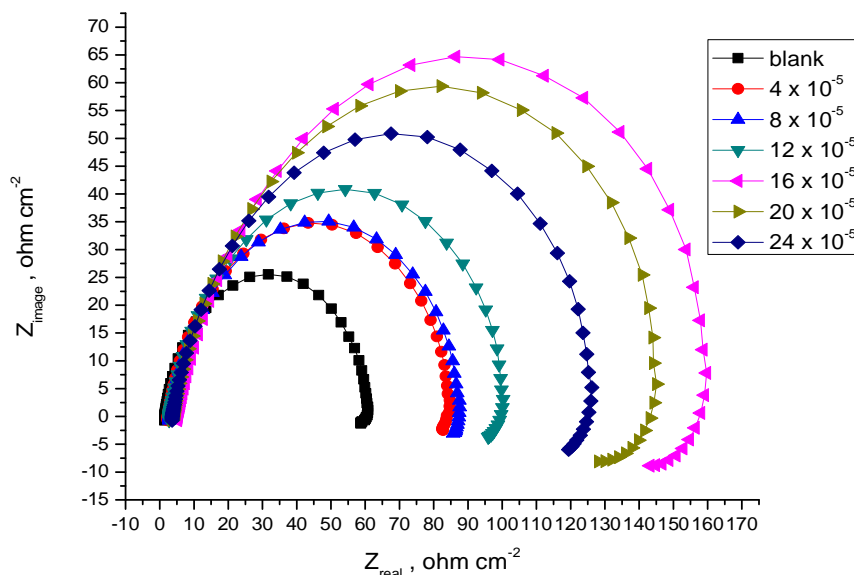


Figure 7. The Nyquist plots for the corrosion of CS in 0.5 M H_2SO_4 in the nonexistence and existence of different doses of compound (A) at 25°C

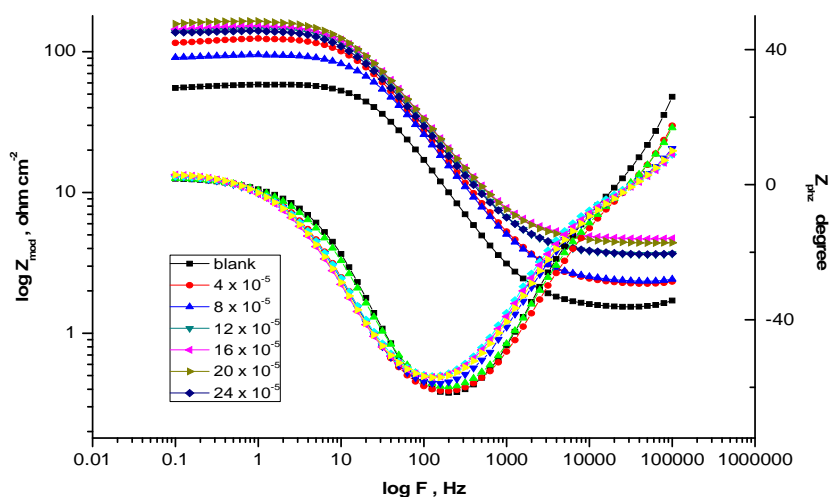


Figure 8: The Bode plots for the corrosion of CS in 0.5 M H_2SO_4 in the nonexistence and existence of different doses of compound (A) at 25°C

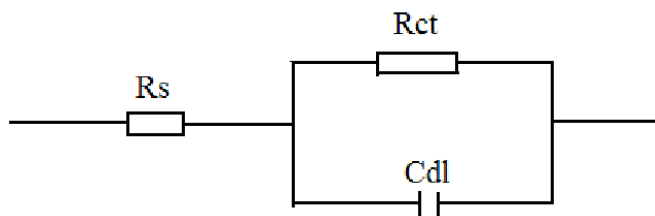


Figure 9: Equivalent circuit used to fit impedance data

Table 7. EIS parameters for the corrosion of CS in 0.5 M H₂SO₄ in the nonexistence and existence of different doses of investigated compound at 25°C

Inhibitor	Conc. $\times 10^5$ M	C_{dl} $\mu F\ cm^{-2}$	R_{ct} $\Omega\ cm^2$	θ	% PE
Blank	0.0	136.6	22.8		
A	4	86.9	82.8	0.72	72.5
	8	84.1	85.4	0.73	73.3
	12	83.6	98.1	0.76	76.8
	16	80.2	128.1	0.82	82.2
	20	79.3	152.4	0.85	85.1
B	24	79.1	166.4	0.86	86.3
	4	76.5	93.2	0.76	75.6
	8	73.4	121.8	0.81	81.3
	12	70.8	138.9	0.83	83.6
	16	62.8	142.8	0.84	84.1
C	20	60.5	148.7	0.84	84.7
	24	59.9	161.9	0.85	85.9
	4	91.1	75.7	0.69	69.9
	8	84.6	96.4	0.76	76.4
	12	80.4	111.9	0.79	79.7
D	16	75.2	113.8	0.80	80.0
	20	74.0	132.8	0.82	82.9
	24	67.8	138.2	0.83	83.5
	4	95.6	40.3	0.43	43.5
	8	94.5	43.2	0.47	47.3
	12	92.4	48.6	0.53	53.1
	16	84.1	53.8	0.57	57.7
	20	80.1	57.9	0.60	60.6
	24	73.6	63.2	0.64	64.0

The results obtained from weight loss, potentiodynamic polarization and impedance techniques are in a good agreement but it is of interest to note that, the values of % PE given by electrochemical techniques are higher than those obtained by weight loss measurements; this may be due to the fact that the electrochemical measurements were carried out on freshly prepared solutions

EFM Measurements: EFM is a nondestructive corrosion measurement like EIS. The great strength of the EFM is the causality factors which serve as an internal check on the validity of the EFM measurement [54]. The results of EFM experiments are a spectrum of current response as a function of frequency. The spectrum is called the inter modulation spectrum. The larger peaks were used to calculate the corrosion current. The % PE calculated from equation 3, it increased with increasing the studied inhibitor doses. Inter modulation spectra obtained from EFM measurements were constructed for iron 0.5 M H₂SO₄ solution in the absence (Figure 10-a) and presence (Figure 10-b) of 2×10^{-4} M of compound (A) at 25°C.

Each spectrum is a current response as a function of frequency; data not shown here. Corrosion kinetic parameters, namely i_{corr} , β_a , β_c and CF-2, CF-3 were listed Table 8 as a function of doses of investigated compounds at 25°C. The causality factors in Table 8, which are very close to theoretical values according to the EFM theory, should guarantee the validity of Tafel slopes and corrosion current densities. The standard values for CF-2 and CF-3 are 2.0 and 3.0, respectively [55].

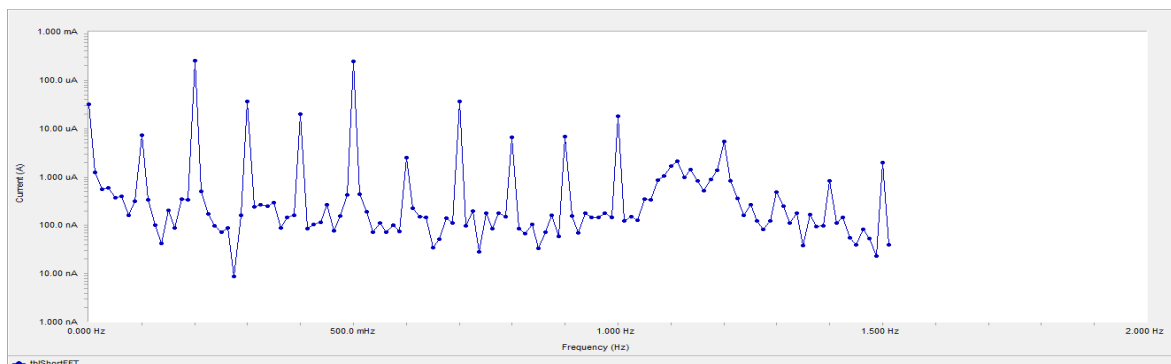


Figure 10-a. EFM spectra for CS in 0.5 M H₂SO₄ (blank)

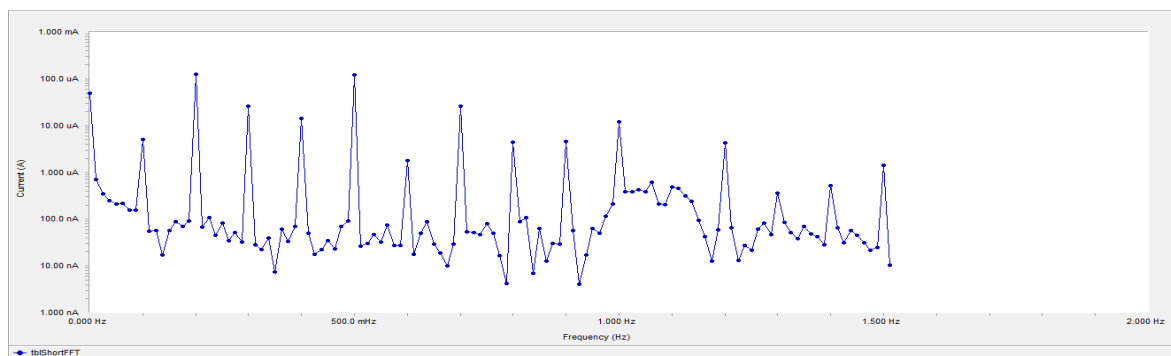


Figure 10-b. EFM spectra for CS in the presence of 2×10^{-4} M inhibitor (A)

Table 8. Electrochemical kinetic parameters obtained from EFM technique for CS in 0.5 M H₂SO₄ in the nonexistence and existence of different doses of investigated compounds

Inh.	[Conc.] M x 10 ⁵	j_{corr} , $\mu\text{A cm}^{-2}$	β_a , m V dec ⁻¹	β_c , mV dec ⁻¹	CF-2	CF-3	C.R.	%PE
Blank	0.0	726.0	57.31	116.7	1.9	3.2	331.7	---
A	4	215.1	55.98	141.7	1.9	3.0	98.3	70.4
	8	212.8	55.43	145.7	1.9	3.3	97.2	70.7
	12	188.7	54.06	152.4	1.9	3.0	86.2	74.0
	16	151.5	52.83	166.2	1.9	2.9	69.2	79.1
	20	140.0	50.98	172.1	1.9	2.9	63.9	80.7
	24	125.7	52.30	169.0	1.9	2.9	57.4	82.7
B	4	376.8	61.41	148.1	1.9	3.0	172.2	48.1
	8	288.8	56.25	143.7	1.9	2.9	131.9	60.2
	12	279.8	53.89	120.1	1.9	3.6	127.9	61.5
	16	252.3	57.24	146.9	1.9	2.9	115.3	65.2
	20	176.2	58.41	165.2	1.9	2.9	80.5	75.7
	24	140.1	54.19	164.5	1.9	2.7	64.0	80.7
C	4	153.5	51.74	154.3	1.9	3.0	70.1	78.9
	8	201.3	54.39	156.3	1.9	3.0	91.9	72.3
	12	129.9	51.93	159.0	1.9	3.0	59.3	82.1

	16	128.5	51.77	160.6	1.9	2.9	58.7	82.3
	20	125.5	53.10	164.3	1.9	2.9	57.3	82.7
	24	116.7	52.81	166.3	1.9	2.9	53.3	83.9
D	4	180.6	108.7	537.4	1.9	3.3	82.5	75.1
	8	173.2	54.83	187.3	1.9	2.9	79.1	76.1
	12	117.0	63.56	176.0	1.9	2.8	53.4	83.9
	16	118.7	57.23	133.7	1.9	3.0	54.2	83.7
	20	116.8	58.12	166.5	1.9	3.1	53.3	83.9
	24	43.06	64.85	161.1	2.0	3.0	19.6	94.1

CONCLUSIONS

In this study, corrosion inhibition efficiency of thiophene derivatives on CS in 0.5 M H₂SO₄ was determined by chemical and electrochemical measurements. EIS data revealed that the values of R_{ct} increases and the values of Cdl decreases by increasing dose of inhibitors. The polarization studies showed that these compounds behave as mixed type inhibitors. These compounds were found to adsorb on CS surface following Langmuir adsorption isotherm.

REFERENCES

- [1] R. Mishra, K.K. Jha, S. Kumar, I.Tomer, *Der Pharma Chemica*, **2011**, 3 (4), 38.
- [2] M.M. Abdou, *Am. J. Chem.*, **2013**, 3, 126.
- [3] I.F.Peperichka, Peperichka D.F., Eds.; John Wiley & Sons: West Sussex Handbook of Thiophene-Based Materials: Applications in Organic Electronics and Photonics, UK, **2009**.
- [4] A. Mishra, C.Q. Ma, P. Bäuerle, *Chem. Rev.*, **2009**, 109, 1141.
- [5] B.S. Ong, Y. Wu, Y. Li, P. Liu, H. Pan, *Chemistry*, **2008**, 14, 4766.
- [6] I. Osaka, R.D. McCullough, *Acc. Chem. Res.*, **2008**, 41, 1202.
- [7] G. Barbarella, M. Melucci, G. Sotgiu, *Adv. Mater.*, **2005**, 17, 1581.
- [8] N.J.L.Guernion, W.Hayes, *Curr. Org. Chem.*, **2004**, 8, 637.
- [9] R.D. McCullough, S. Hotta, K.Ito, P.Bäuerle, D. Fichou, C. Ziegler, G. Horowitz, P. Delannoy, J. Cornil, D. Beljonne, Handbook of Oligo- and Polythiophenes; Fichou, D.Ed.;Wiley-VCH: Weinheim, Germany, **1999**.
- [10] H.S.O. Chan, S.C. Ng, *Prog. Polym. Sci.*, **1998**, 23, 1167.
- [11] G.Schopf, G.Komehl, In Advances in Polymer Sciences: Polythiophenes-Electrically Conductive Polymers; Ed. Springer-Verlag: Berlin, Germany, **1997**.
- [12] J. Roncali, *Chem. Rev.*, **1992**, 92, 711.
- [13] R.J. Angelici, *Organometallics*, **2001**, 20, 1259.
- [14] T.B. Rauchfuss, *Prog. Inorg. Chem.*, **1991**, 39, 259.
- [15] G. Roman, *Org. Chem.*, **2013**, 10, 27
- [16] G. Rassu, F. Zanardi, L. Battistini, G. Casiraghi, *Chem. Soc. Rev.*, **2000**, 29, 109.
- [17] S. Elayyoubi, E.B. Maarouf, H. Oudda and B. Hammouti, *Bull. Electrochem.*, **2002**, 18, 45.
- [18] A. Ouchrif, A. Yahyi, B. Hammouti, A. Dafali, M. Benkaddour and A. Et-Touhami, *Bull. Electrochem.*, **2003**, 19, 455.
- [19] M. Bouklah, B. Hammouti, A. Aouniti and T. Benhadda, *Prop. Org. Coat.*, **2004**, 47, 225.
- [20] G. Y. Elewad, *Inter.J. Electrochem. Sci.*, **2008**, 3, 1149.
- [21] I. Zaafarany, M. Abdallah, *Inter.J. Electrochem. Sci.*, **2010**, 5(1), 18.
- [22] A. Yurt, A. Balaban, S. U. Kandemir and G. Bereket, *Mater. Chem. Phys.*, **2004**, 85(2-3), 420.
- [23] S. A. Ali, H. A. Al-Muallema, S. U. Rahman, M. T. Saeed, *Corros. Sci.*, **2008**, 50(11), 3070
- [24] H. Ju, Z. P. Kai, and Y. Li, *Corros. Sci.*, **2008**, 50(3), 865.
- [25] D. I. Gopi, K. Govindaraju, L. Kavhith, *J. Appl. Electrochem.*, **2010**, 40(7), 1349.
- [26] M. A. Migahed, A. M. Abdul-Raheim, A. M. Atta, W. Brostow, *Mater. Chem. Phys.*, **2010**, 121(1-2), 208.

- [27] A. Singh, M. Quraish, *Journal of Appl. Electrochem.*, **2010**, 40(7), 1293.
[28] I. B. Obot, N. O. Obi-Egbedi, N. W. Odozi, *Corros. Sci.*, **2010**, 52(3), 923.
[29] I. B. Obot and N. O. Obi-Egbedi, *Mater. Chem. Phys.*, **2010**, 122(2-3), 325.
[30] H. Ashassi-Sorkhabi, M. Es'haghi, *J.Solid State Electrochem.* **2009**, 13(8), 1297.
[31] A.A.Al-Sarawy, A.S.Fouda, W.A.S.El-Dein, *Desalination*, **2008**, 229(1-3), 279.
[32] J.M. Abdel Kader, A.M. Shams El Din, *Corros. Sci.*, **1970**, 10, 551.
[33] S.S. Sampat, J.C. Vora, *Corros. Sci.*, **1974**, 14, 591.
[34] L.A. Shalaby, K.M. El Sobki, A.A. Abdel Azim, *Corros. Sci.*, **1976**, 16, 637.
[35] G.A. El Mahdy, S.S. Mahmoud, *Corros. Sci.*, **1995**, 51, 436.
[36] N.C. Subramanyam, B.S. Sheshardi, S.M. Mayanna, *Corros. Sci.*, **1993**, 34,563
[37] F. Bentiss, M. Traisnel, M. Lagene, *Corros. Sci.*, **2000**, 42, 127.
[38] S. Huang, Y. Pan, Y. Zhu, A. Wu, *Org. Lett.*, **2005**, 7, 3797.
[39] J. Aljourani, M.A. Golozar, K. Raessi, *Mater. Chem. Phys.*, **2010**, 121(1-2), 320.
[40] P.O.Ameh and N.O.Eddy, *Res.Chem. Intermediates*, **2014**, 40(8), 2641.
[41] A. Petchiammal, R.P.Deepa, S. Selvaraj, K.Kalirajan. *Res. J. Chem. Sci.*, **2012**, 2(4), 24.
[42] A. S. Fouda, A A.l-Sarawy E. El-Katori, *Desalination*, **2006**, 201, 1.
[43] G. Gece., *Corros. Sci.*, **2008**, 50, 2981.
[44] Tang L, LPEX, SiY, MuG. And LiuG, *Mater. Chem. Phys.*, **2006**, 95, 29.
[45] Tang L, Murad G. and LiuG, *Corros. Sci.*, **2003**, 45, 2251.
[46] S.S. Abdel-Rehim, K.F. Khalid, N.S.Abd-Elshafi, *Electrochim. Acta*, **2006**, 51, 3269.
[47] E. Khamis, *Corrosion (NACE)*, **1990**, 46, 476.
[48] LiX. and TangL, *Mater. Chem. Phys.*, **2005**, 90, 286.
[49] A. A.El-Awady, B.Abd El-Nabey, S. G.Aziz, *Electrochem. Soc.*, **1992**, 139, 2149.
[50] S. S.Abd El-Rehim, H.H.Hassan and M. A.Amin, *Mater.Chem. Phys.*, **2001**, 70, 64.
[51] A. K.Singh, M. A.Quraishi, *Corros. Sci.*, **2010**, 52, 1373.
[52] F.Bentiss, C.Jama, B.Mernari, E.Attari, H. E .KadiL., M. Lebrini, M. Traisnel, M. Lagrenee, *Corros. Sci.*, **2009**, 51, 1628.
[53] Ashassi-Sorkhabi H, Seifzadeh D, Hosseini M.G, *Int. J. Electrochem. Sci.*, **2008**, 9, 20143.
[54] A.Popova and M.Christov, *Corros. Sci.*, **2006**, 48, 3208.
[55] Gamry Echem Analyst Manual, **2003**.

AUTHOR ADDRESS

1. A. S. Fouda

Department of Chemistry,
Faculty of Science,
Mansoura University,
Mansoura-35516, Egypt
E-mail:asfouda@hotmail.com,
Tel: +2 050 2365730, Fax: +2 050 2365730